1521-009X/51/4/492–498$35.00
DRUG METABOLISM AND DISPOSITION

dx.doi.org/10.1124/dmd.122.001111
Drug Metab Dispos 51:492–498, April 2023

CYP3A4 and *CYP3A5* Expression is Regulated by *CYP3A4*1G* in CRISPR/Cas9-Edited HepG2 Cells[S]

Weihong Yang, Huan Zhao, Yaojie Dou, Pei Wang, Qi Chang, Xiaomeng Qiao, Xiaofei Wang, Chen Xu, Zhe Zhang, and Lirong Zhang

Department of Forensic Medicine (W.Y., H.Z., Y.D., X.Q., C.X.) and Department of Pharmacology (P.W., Q.C., X.W., L.Z.), School of Basic Medical Sciences, Zhengzhou University, Zhengzhou, China; and Department of Gastroenterology, the Second Affiliated Hospital of Zhengzhou University, Zhengzhou, China (Z.Z.)

Received September 10, 2022; accepted December 5, 2022

ABSTRACT

Functional *CYP3A4*1G* (G>A, rs2242480) in cytochrome P450 *3A4* (*CYP3A4*) regulates the drug-metabolizing enzyme *CYP3A4* expression. The objective of this study was to investigate whether *CYP3A4*1G* regulates both basal and rifampicin (RIF)-induced expression and enzyme activity of *CYP3A4* and *CYP3A5* in gene-edited human HepG2 cells. *CYP3A4*1G* GG and AA genotype HepG2 cells were established using the clustered regularly interspaced short palindromic repeats/CRISPR-associated protein 9 (CRISPR/Cas9) single nucleotide polymorphism technology and homology-directed repair in the *CYP3A4*1G* GA HepG2 cell line. In *CYP3A4*1G* GG, GA, and AA HepG2 cells, *CYP3A4*1G* regulated expression of *CYP3A4* and *CYP3A5* mRNA and protein in an allele-dependent manner. Of note, significantly decreased expression level of *CYP3A4* and *CYP3A5* was observed in *CYP3A4*1G* AA HepG2 cells. Moreover, the results after RIF treatment showed that *CYP3A4*1G* decreased the induction level of *CYP3A4* and *CYP3A5* mRNA expression in *CYP3A4*1G* AA HepG2 cells. At the same time, *CYP3A4*1G* decreased CYP3A4 enzyme activity and tacrolimus metabolism, especially in *CYP3A4*1G* GA HepG2 cells. In summary, we successfully constructed *CYP3A4*1G* GG and AA homozygous HepG2 cell models and found that *CYP3A4*1G* regulates both basal and RIF-induced expression and enzyme activity of *CYP3A4* and *CYP3A5* in CRISPR/Cas9 *CYP3A4*1G* HepG2 cells.

SIGNIFICANCE STATEMENT

Cytochrome P450 (*CYP*) *3A4*1G* regulates both basal and rifampicin (RIF)-induced expression and enzyme activity of *CYP3A4* and *CYP3A5*. This study successfully established *CYP3A4*1G* (G>A, rs2242480), GG, and AA HepG2 cell models using CRISPR/Cas9, thus providing a powerful tool for studying the mechanism by which *CYP3A4*1G* regulates the basal and RIF-induced expression of *CYP3A4* and *CYP3A5*.

Introduction

In human adult livers, cytochrome P450 3A (CYP3A) and its major components, CYP3A4 and CYP3A5, play a crucial role in clinical drug metabolism, by metabolizing more than 60% of clinical prescription drugs. Genetic variation in *CYP3A4*, such as the single nucleotide polymorphism (SNP) *CYP3A4*22* (rs35599367, G>A) in intron 6, which affects its transcript splicing, decreases *CYP3A4* expression (Wang and Sadee, 2016), resulting in improved pharmacokinetics and clinically effective therapy (Wang et al., 2011 Mulder et al., 2021). The intronic genetic variation in *CYP3A5*, *CYP3A5*3* (rs776746, A>G), leads to decreased normal *CYP3A5* expression through alternative splicing (Kuehl et al., 2001) and is associated with tacrolimus dosage and pharmacokinetics (Dorr et al., 2017; Tang et al., 2019). Recently, these two SNPs have become biomarkers for clinical individualized medications. Therefore, elucidating the mechanisms of individual differences in CYP3A enzyme activity from the perspective of intron SNP variation can provide new ideas for the implementation of precise and individualized treatments. Interestingly, another important *CYP3A4* variation, *CYP3A4*1G* (rs2242480, G>A) (Fig. 1), is an intronic SNP enhancer (He et al., 2011; Yang et al., 2015) that is suspected to be a vital SNP in regulation of *CYP3A4* expression and enzyme activity.

*CYP3A4*1G* is associated with the metabolism of numerous drugs (Gao et al., 2008; Zhang et al., 2010; Yuan et al., 2011; Dong et al., 2012; Ren et al., 2015; Yuan et al., 2015; Zhang et al., 2017; Lv et al., 2018; Zhang et al., 2018). CYP3A5 and CYP3A4 have highly substrate similarity, and CYP3A5 can metabolize most of substrates metabolized by CYP3A4. *CYP3A5*3*, which causes protein truncation, results in the absence of normal *CYP3A5* expression, while *CYP3A5*1* is related to normal *CYP3A5* expression. Although *CYP3A5*3* linkage with *CYP3A4*1G* might interfere with the metabolism of drugs metabolized by CYP3A4, the relation between *CYP3A4*1G* and tacrolimus in *CYP3A5* expressers, or atorvastatin in *CYP3A5* non-expressers, were further confirmed (Miura et al., 2011; He et al., 2014; Liu et al., 2017). Moreover, the allele frequency of *CYP3A4*1G* highly differs between ethnic lines, and its global allele frequency is about 0.15 (ranging between about 0.09 and 0.86 among 11 populations). Nine out of the eleven populations

This work was supported by the National Natural Science Foundation of the People's Republic of China [Grant Number 81773815] and by the Project of Science and Technology Department of Henan Province of China [Grant Number 222102310186 and 162102310523].

No author has an actual or perceived conflict of interest with the contents of this article.

dx.doi.org/10.1124/dmd.122.001111.

[S] This article has supplemental material available at dmd.aspetjournals.org.

ABBREVIATIONS: CRISPR/Cas9, clustered regularly interspaced short palindromic repeats/CRISPR-associated protein 9; *CYP3A4*, cytochrome P450 *3A4*; EGFP, enhanced green fluorescent protein; ER6, everted repeat sequence separated by 6 bp; HDR, homology-directed repair; PCR, polymerase chain reaction; px330, PX330a-42230; PXR, pregnane X receptor; RIF, rifampicin; sgRNA, single guide RNA; SNP, single nucleotide polymorphism.

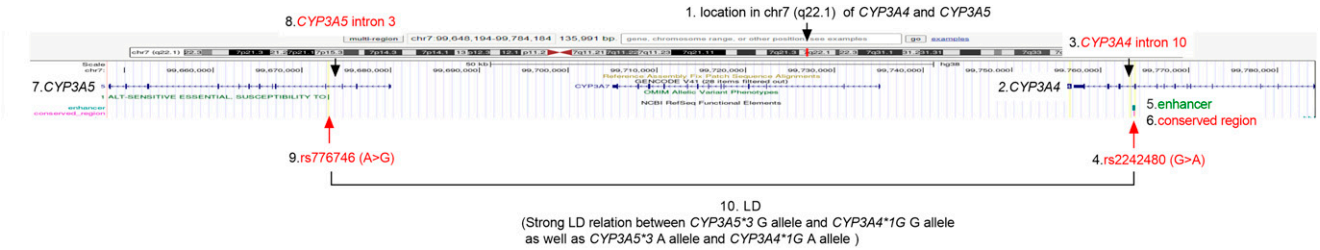

Fig. 1. The location of *CYP3A4*1G*, *CYP3A5*3* and their linkage disequilibrium relation Rs2242480 and rs776746 indicate *CYP3A4*1G* and *CYP3A5*3*, respectively.

have allele frequencies over 0.28 (https://www.ncbi.nlm.nih.gov/snp/rs2242480#frequency_tab). Using luciferase enhancer reporter assays, we previous showed that *CYP3A4*1G*, in the full-length of *CYP3A4* intron 10, as an enhancer, regulates the expression of *CYP3A4* (Yang et al., 2015). However, since suitable *CYP3A4*1G* cell models are unavailable due to *CYP3A4*1G* strong linkage with *CYP3A5*3* (Fig. 1), the mechanism is not clear. It is still unclear whether the enhancer, *CYP3A4*1G*, regulates *CYP3A4* expression and enzyme activity in the native chromatin context of *CYP3A4*1G* in living cells of different genotypes, as reporter gene assays inherently disconnect regulatory elements from their target genes and may not reflect in-vivo activity (Bu and Gelman, 2007; Kato et al., 2007; Wang et al., 2008). Now, precision SNP clustered regularly interspaced short palindromic repeats/CRISPR-associated protein 9 (CRISPR/Cas9) mediated homology-directed repair (HDR) technology is available (Hegde et al., 2021). Thus, the establishment of a human *CYP3A4*1G* liver cell line by CRISPR/Cas9 technology may lay the foundation to explore the relationship between the intronic SNP variation of *CYP3A4* gene, its regulatory mechanism, and drug metabolism.

HepG2 cells, a hepatoblastoma cell line derived from human liver tissue of a 15-year-old white male from the Caucasian region (López-Terrada et al., 2009), are commonly used for in vitro drug metabolism studies. The genotypes of *CYP3A4*1G*, *CYP3A5*3*, and *CYP3A4*22* in HepG2 cells are GA, AG, and CC, respectively (Zhao and Zhang, 2016). Therefore, HepG2 cells are suitable for being edited to *CYP3A4*1G* GG and AA HepG2 cell strains. In HepG2 cells, as *CYP3A5*3* is highly linked with *CYP3A4*1G*, we speculated *CYP3A4*1G* was related to *CYP3A5* expression and enzyme activity. Rifampicin (RIF), as a strong inducer, can increase *CYP3A4* expression through the pregnane X receptor (PXR). However, it is not clear whether RIF may induce the expression of *CYP3A* in gene-edited *CYP3A4*1G*, GG, and AA HepG2 cells.

In this study, we established *CYP3A4*1G*, GG, and AA HepG2 cell strains successfully using CRISPR/Cas9 technology. We further verified that *CYP3A4*1G* regulated both basal and RIF-induced expression, and the metabolism of *CYP3A4* and *CYP3A5* in *CYP3A4*1G* HepG2 cells. These findings will enrich the basic theory that *CYP3A4* intron enhancer SNP regulates the expression and enzyme activity of *CYP3A4* and *CYP3A5* and provide a new idea for accounting for the variability of CYP3A activity and clinical precision medicine.

Materials and Methods

Cell Lines

HepG2 and HEK293T cells were obtained from Stem Cell Bank, Chinese Academy of Sciences (Shanghai, China) and cultured in a high-sugar Dulbecco's modified Eagle's medium medium supplemented with 10% fetal bovine serum, 100 U/ml penicillin, and 100 μ g/ml streptomycin at 37°C with 5% CO_2.

Establishment of *CYP3A4*1G* GG and AA HepG2 Cells by CRISPR/Cas9

Construction and Identification of px330 and pmCherry Enhanced Green Fluorescent Protein (EGFP) Reporter Recombination Plasmids. According to human *CYP3A* GenBank AF280107.1 from the National Center for Biotechnology Information, single guide RNA (sgRNA), pmCherry EGFP reporter sequences, and HDR template containing *CYP3A4*1G* G or A allele were designed by software ZiFiT and Vector NTI 11.5.1, respectively. PX330a-42230 (px330) and pmCherry EGFP reporter vectors were kindly donated by Professor Yaohe Wang of the Sino-British Research Centre for Molecular Oncology, National Centre for International Research in Cell and Gene Therapy, Academy of Medical Sciences, Zhengzhou University. The above sgRNA and pmCherry EGFP reporter sequences (Fig. 2, Supplemental Table 1) were synthesized (Shanghai Shenggong Co., Ltd, China) and inserted to px330 and pmCherry EGFP reporter vectors and verified by enzyme digestion and sequencing (Shanghai Shenggong Co., Ltd).

Establishment of *CYP3A4*1G* GG and AA HepG2 Cell Strains. To achieve *CYP3A4*1G* wild-type (GG) and mutant type (AA), homozygous HepG2 cells, CRISPR/Cas9 mediated HDR templates (Supplemental Table 1) were synthesized (Jinsirui Biotechnology Co., Ltd., Nanjing, China). The above px330-sgRNA, pmCherry EGFP reporter recombinant vectors along with the corresponding HDR templates were co-transfected into *CYP3A4*1G* GA HepG2 cells using Lipofectamine 2000 (Thermo Fisher Scientific, Carlsbad, CA, USA) following the manufacturer's instructions. Higher efficiency px330-sgRNA (1.5 μg), pmCherry EGFP-reporter (1.5 μg) and corresponding HDR templates (10 μM, 5 μl) were used according to the proportion 1:3 of DNA (μg): Lipofectamine 2000 (μl). Forty-eight hours post transfection in six-well plates, the objective HepG2 cells were collected and sorted using the BD FACSCanto flow cytometry instruments from BD Biosciences (San Jose, CA, USA) and cultured in monoclonal cell way into 96-well plates. Finally, their genomic DNA was extracted and polymerase chain reaction (PCR) amplified. The PCR products were sequenced to screen *CYP3A4*1G* GG and AA monoclonal HepG2 cell strains. Primers used are shown (Supplemental Table 2).

Validation of Off-Target Objective HepG2 Cell Strains. To ensure there were potential off-target sites of the sgRNA-2W and sgRNA-3M in screened *CYP3A4*1G* GG and AA HepG2 cells, the potential off-target gene sequence and its location on chromosome (Supplemental Table 3) were predicted. Primers for several predicted top off-target locations (Supplemental Table 3) were designed online (https://zlab.bio/guide-design-resources), and off-target situations in above HepG2 cells were evaluated by sequencing of PCR products.

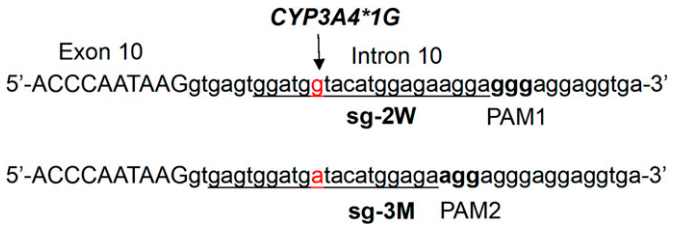

Fig. 2. *CYP3A4*1G* allele (rs2242480) and guide RNA targeting strategy Guide RNAs were targeted to protospacer adjacent motif sequences on same side of the *CYP3A4*1G* allele (sg-2W and sg-3M locus). *CYP3A4* exon 10 sequence is in capital letters, and the downstream intron 10 sequence is in lowercase letters.

Examination of Basal Expression of *CYP3A4* and *CYP3A5* mRNA and Protein mRNA Analysis. Total RNA was extracted from *CYP3A4*1G* GG, GA, and AA HepG2 cells using TRizol Reagent (TIANGEN, Beijing, China) according to the manufacturer's instructions. cDNA was reverse transcribed from total RNA, and 5 ng of cDNA was amplified using an iQ5 Real-Time PCR Detection System with SYBR Green Master Mix from Thermo Fisher Scientific. Primers used are shown in Supplemental Table 2. The relative expression of *CYP3A4, CYP3A5,* and *PXR* was calculated by $2^{-\triangle\triangle Ct}$ method, and normalized to *glyceraldehyde-3-phosphate dehydrogenase*.

Western Blot Analysis. Total proteins of the above *CYP3A4*1G* GG, GA, and AA HepG2 cells were prepared using RIPA buffer. Protein concentrations were determined by BCA Protein Assay. Protein samples were separated by 12% SDS polyacrylamide gel electrophoresis and transferred to polyvinylidene difluoride membranes. The membranes were blocked with 5% non-fat dried milk in 1×tris buffered saline, 0.1% Tween-20 and incubated overnight with primary antibodies for CYP3A4 or CYP3A5-(Abcam) at 1/1000 dilution. The next day, the membranes were incubated in horseradish peroxidase-labeled secondary antibodies and visualized with an enhanced chemiluminescence method. Anti-glyceraldehyde-3-phosphate dehydrogenase (Abcam) at 1/5000 was used as a loading control.

Detection of *CYP3A4* and *CYP3A5* Induction Expression

*CYP3A4*1G* GG, GA, and AA HepG2 cells cultured in 12-well plates were treated with 10 μM RIF (Sigma-Aldrich, St. Louis, MO) for 48 hours prior to harvesting, *CYP3A4, CYP3A5,* and *PXR* mRNA expression levels were examined by quantitative real-time polymerase chain reaction.

CYP3A4 Enzyme Activity and Tacrolimus Metabolism Study

P450-Glo CYP3A4 Assay. *CYP3A4*1G* GG, GA, and AA HepG2 cells were washed with phosphate-buffered saline and luminescence was measured using the P450-Glo CYP3A4 assay kit and Luciferin-IPA (Promega, Cat # V9001) with a plate reader as previous described (Pande et al., 2020).

Tacrolimus Metabolism Assays. *CYP3A4*1G* GG, GA, and AA HepG2 cells were treated with tacrolimus and incubated for 24 hours. Tacrolimus from Dalian Meilun Biotechnology Co., Ltd. (Shanghai, China) was diluted in methanol (1 mg/ml) so that tacrolimus final concentration in cell culture medium was 50 ng/ml. Media were collected and assayed for tacrolimus by ultra-high-performance liquid chromatography-mass spectrometry system according to previously described methods with minor modifications (Dorr et al., 2017; Liu et al., 2020; Shi et al., 2022). Collected media were centrifuged, and 40 μl of supernatant with 160 μl of glacial acetonitrile were vortexed for 30 seconds and placed on ice for 20 minutes before being centrifuged again. The supernatants were dried and resuspended in 320 μl of methanol and mixed with 40 μl of internal standard (ascomycin, 2000 ng/ml, dissolved in methanol) from Dalian Meilun Biotechnology Co., Ltd. (Shanghai, China). After vortexing and centrifugation at 14,000×g for 30 minutes at 4°C, the supernatants were filtered with a membrane and placed in a liquid injection flask. The residual amount of tacrolimus in the sample was determined using ultra-high-performance liquid chromatography-mass spectrometry including Shimadzu LC-30A system and 6500 QTRAP triple quadrupole mass spectrometer equipped with an ESI source) (ABSCIEX, USA). The mobile phase A was ammonium acetate aqueous solution, and mobile phase B was methanol. Loading volume was 3 μl. An Atlantis T3 column (2.1 mm × 100 mm, 3 μm) was used, and the column temperature was 40°C. The transitions (precursor to product) monitored are m/z 821.7 to 768.5 for tacrolimus and m/z 809.7 to 729.6 for the internal standard, respectively. Ionization was performed in positive ion mode with a capillary voltage of 5.5 kV, a cone voltage of 61/74 (tacrolimus/internal standard), an ion source temperature of 550°C, and a collision gas pressure of 27.8/21 V (tacrolimus/internal standard).

Statistical Analysis

Statistical analysis was performed using Statistical Product and Service Solutions 21.0 software (IBM, Armonk, NY, USA). All comparisons were conducted using one-way or two-way ANOVA with Bonferroni post hoc test. Data were shown as mean ± S.D. $P < 0.05$ was considered statistically significant.

Results

Establishment of *CYP3A4*1G* GG and AA HepG2 Cells by CRISPR/Cas9 Technology

Identification of px330 and pmCherry EGFP Reporter Recombination Plasmids. Sequencing results verified the correctness of the sequences and directions of positive recombination plasmids, px330-sgRNA, and pmCherry EGFP reporter with inserted target fragment sequences (Supplemental Fig. 1, A and B).

Identification of Gene-Edited *CYP3A4*1G* GG and AA HepG2 Cells. The efficiency of the sgRNA expression vector was screened in HEK293T cells (Supplemental Fig. 1C). To construct *CYP3A4*1G*, GG, and AA HepG2 cells, objective px330-sgRNA, pmCherry EGFP reporter recombinant vectors and the corresponding homologous recombination repair templates were co-transfected into *CYP3A4*1G* GA HepG2 cells. Monoclonal cells of the objective HepG2 cells were sorted and cultured. Identification of gene-edited *CYP3A4*1G* GG and AA HepG2 cells was performed by genomic DNA extraction, PCR amplification, and sequencing. Results of sequencing indicated that the genotypes of objective *CYP3A4*1G* GG and AA HepG2 cell strains were both homozygous compared with *CYP3A4*1G* GA HepG2 cells (Fig. 3). In *CYP3A4*1G* GG HepG2 cells the sequencing alignment (Supplemental Fig. 2A) unexpectedly revealed a deletion of two continuous bases (GA) at the ninth and tenth sites downstream of the *CYP3A4*1G* G allele in *CYP3A4* intron 10. For *CYP3A4*1G* AA HepG2 cells, there was one base deletion in 11th base (A) downstream of the *CYP3A4*1G* A allele. Above all, the *CYP3A4*1G* point mutation was correctly edited, and the *CYP3A4*1G* wild-type and mutant homozygote HepG2 cell strains were successfully constructed.

Off-Target Effects Validation of Monoclonal Cells. Genomic DNA of *CYP3A4*1G* GG, GA, and AA HepG2 cells was subjected to PCR and sequencing using off-target primers. Comparing the sequencing results with the predicted off-target sequences showed eight sequences without off-target (Supplemental Fig. 3, A and B), and two near sequences, 3M-2 and 2W-1, off-target in these ten sequences. The off-target sequence in *CYP3A4*1G* GG HepG2 was the second sequence, 3M-2 GAGTGGA**CA**GTACATGGAGAA on chr7: -99710713 predicted by sgRNA-3M, where there was a base A insertion, highlighted by underline (Supplemental Fig. 2B). In *CYP3A4*1G* AA HepG2, the off-target sequence very near 3M-2 was the first sequence, 2W-1 GGA**CA**G-TACATGGAGAAGGA on chr7: -99710709 predicted by sgRNA-2W, where there was a 14 bp deletion, shown by underlined sequence, on chr7 (99710723-99710710) *CYP3A7* intron 10, as well as four SNP homozygous mutations in *CYP3A7* exon 10 (Supplemental Fig. 2B). The genotypes of these SNPs were rs754782383 (T>C) CC 90th, rs777212283 (C>T) new mutation C>G GG 127th, rs1336177699 (T>G) new mutation T>C CC 133rd, and rs756922005 (T>C) CC 145th in exon 10 of *CYP3A7*. *CYP3A4*1G* GG and AA HepG2 were used for further study.

*CYP3A4*1G* regulates basal expression of *CYP3A4* and *CYP3A5*

Basal expression levels of *CYP3A4* and *CYP3A5* mRNA and protein in *CYP3A4*1G* GG, GA and AA HepG2 cells were examined by quantitative real-time polymerase chain reaction and western blot. *CYP3A4* mRNA expression levels decreased in *CYP3A4*1G* AA HepG2 cells compared with *CYP3A4*1G* GG and GA HepG2 cells (both $P < 0.01$), and *CYP3A4* mRNA expression in *CYP3A4*1G* GA HepG2 cells was lower than that in *CYP3A4*1G* GG HepG2 cells ($P < 0.01$) (Fig. 4A). Moreover, CYP3A4 protein expression level also decreased in *CYP3A4*1G* AA HepG2 cells compared with *CYP3A4*1G* GG ($P < 0.01$) and GA HepG2 cells, despite the fact that there was no significant difference between *CYP3A4*1G* AA and GA HepG2 cells (Fig. 4B). These results indicate that *CYP3A4*1G* regulates the mRNA and protein expression levels of *CYP3A4* in an allele-dependent manner. As *CYP3A5*3*

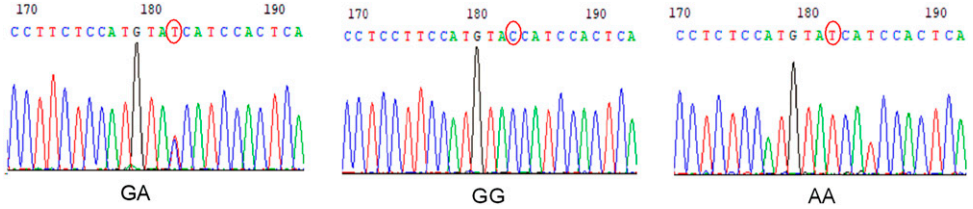

Fig. 3. Sequencing results of gene-edited *CYP3A4*1G* HepG2 cells. GA, GG, and AA indicate sequencing results of *CYP3A4*1G* GA, GG, and AA HepG2 cells, respectively. *CYP3A4*1G* GA HepG2 cells are the control. A base with a red circle in the sequence shows the *CYP3A4*1G* site and corresponding genotype.

showed linkage with *CYP3A4*1G*, *CYP3A5* mRNA and protein expression levels were also examined. Similarly, *CYP3A4*1G* also regulated *CYP3A5* mRNA and protein expression in an allele dependent-manner (Fig. 4, C and D). *CYP3A5* mRNA expression level in *CYP3A4*1G* AA HepG2 cells was lower than that in *CYP3A4*1G* GG HepG2 cells ($P < 0.01$), and there was a significant difference for *CYP3A5* mRNA expression level between *CYP3A4*1G* GA and GG HepG2 cells ($P < 0.05$) (Fig. 4C). The protein expression levels of CYP3A5 were also lower in *CYP3A4*1G* AA HepG2 cells than that in *CYP3A4*1G* GG and GA HepG2 cells ($P < 0.01$ or $P < 0.05$), and there was also a significant difference for CYP3A5 protein expression levels between *CYP3A4*1G* GA and GG HepG2 cells ($P < 0.05$) (Fig. 4D). In summary, *CYP3A4*1G* regulates basal expression of *CYP3A4* and *CYP3A5* at both mRNA and protein levels.

*CYP3A4*1G* Decreases RIF-Induced Expression of *CYP3A4* and *CYP3A5*

RIF, a strong inducer of CYP3A4 enzyme, can induce *CYP3A4* expression by PXR; therefore, we investigated the impacts of *CYP3A4*1G* on the RIF-induced *CYP3A4* and *PXR* expression in different *CYP3A4*1G* HepG2 cells. As shown in Fig. 5A, RIF could induce the *CYP3A4* mRNA expression levels in *CYP3A4*1G* GG, GA, and AA HepG2 cells, as compared with the control group ($P < 0.01$ or $P < 0.05$). However, diminished induction levels of *CYP3A4* by RIF were observed in the *CYP3A4*1G* AA and GA HepG2 cells as compared with the *CYP3A4*1G* GG HepG2 cells. RIF increased *CYP3A4* mRNA expression in the above three different *CYP3A4*1G* genotype HepG2 cells in an allele-dependent manner as compared with the DMSO alone control groups, with the induction of *CYP3A4*1G* AA and GG HepG2 cells being the weakest and the strongest (over 6-fold *CYP3A4* mRNA expression), respectively. The roles of induction of RIF in *CYP3A4*1G* GA HepG2 cells were between them. These results suggest that RIF induces *CYP3A4* mRNA expression in *CYP3A4*1G* allele-dependent manner.

*CYP3A4*1G* also affected *CYP3A5* mRNA expression; therefore, we analyzed whether RIF could also induce *CYP3A5* expression. Similar to *CYP3A4* induction by RIF, *CYP3A4*1G* decreased *CYP3A5* mRNA expression. Comparing the same *CYP3A4*1G* genotype HepG2 cells between RIF and DMSO groups, *CYP3A5* mRNA expression was also all increased after RIF treatment; however, the extent of induction of RIF in *CYP3A4*1G* AA HepG2 cells was much lower than that in *CYP3A4*1G* GG and GA HepG2 cells. There was significant difference in *CYP3A4*1G* GG or GA HepG2 cells after being induced ($P < 0.01$ or $P < 0.05$). RIF induction in *CYP3A4*1G* GG HepG2 cells was over

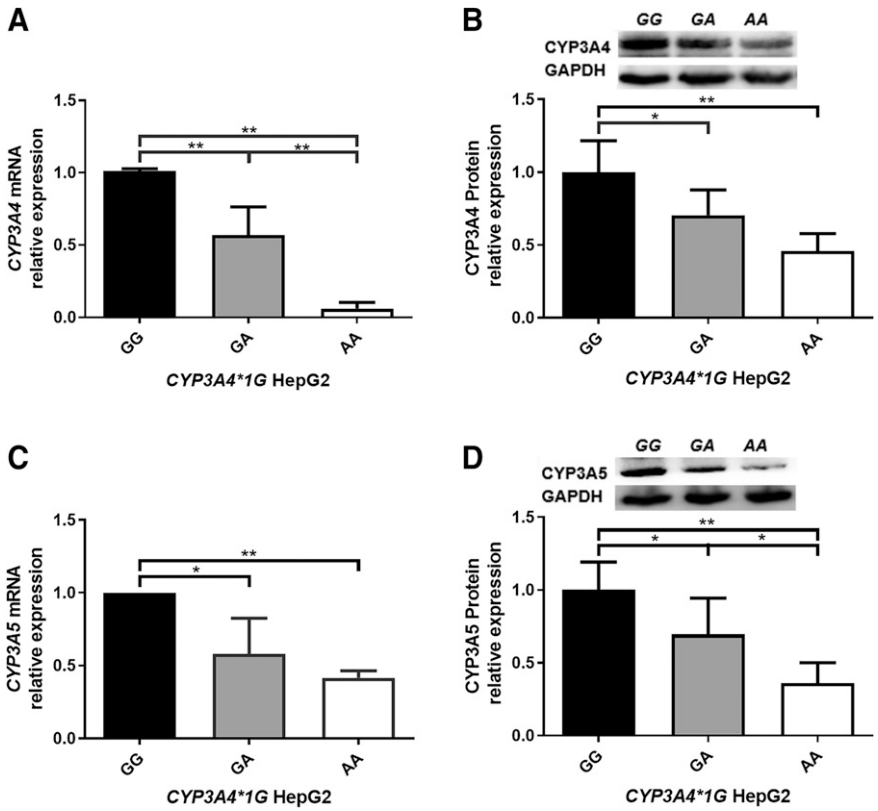

Fig. 4. *CYP3A* basal expression in *CYP3A4*1G* GG, GA, and AA HepG2 cells. *CYP3A4* mRNA (A) and protein (B) expression levels in *CYP3A4*1G* GG, GA, and AA HepG2 cells. *CYP3A5* mRNA (C) and protein (D) expression levels in *CYP3A4*1G* GG, GA, and AA HepG2 cells. The error bars represent S.D. (n = 3 per group for mRNA and protein). (*$P < 0.05$, **$P < 0.01$)

6-fold that of the *CYP3A5* mRNA expression of the same genotype HepG2 cells in the DMSO group (Fig. 5B). These results indicate that RIF also induces *CYP3A5* mRNA expression in a *CYP3A4*1G* allele-dependent manner, and its induction level in *CYP3A4*1G* AA HepG2 cells is much lower than that in *CYP3A4*1G* GG HepG2 cells.

Since RIF induced *CYP3A4* by PXR, PXR mRNA expression levels in different *CYP3A4*1G* genotype HepG2 cells were also determined. Comparing *PXR* expression between the DMSO and RIF group, we found that *PXR* mRNA expression level in *CYP3A4*1G* GG HepG2 cells was much higher in the RIF group than that in the DMSO group ($P < 0.05$); however, *PXR* mRNA expression levels in the other genotype HepG2 cells were not significantly increased (Fig. 5C). Particularly, diminished basal and RIF-induced mRNA expression levels of *PXR* were observed in the *CYP3A4*1G* AA (both $P < 0.05$) and GA HepG2 cells (both $P < 0.05$) as compared with the *CYP3A4*1G* GG HepG2 cells. These results reveal that *CYP3A4*1G*-decreases basal and RIF-induced mRNA expression levels of *PXR*.

*CYP3A4*1G* Affects CYP3A4 and CYP3A5 Activity in HepG2 Cells

To further study the effects of *CYP3A4*1G* on enzyme activity of CYP3A4 and CYP3A5, CYP3A4 enzyme activity and tacrolimus metabolism were also evaluated. CYP3A4 enzyme activity decreased in *CYP3A4*1G* AA and GA HepG2 cells compared with *CYP3A4*1G* GG HepG2 cells, and CYP3A4 enzyme activity in *CYP3A4*1G* GA HepG2 cells was the lowest of the three (both $P < 0.01$) (Fig. 6A). Similarly, for CYP3A5 metabolism, the amount of tacrolimus metabolized in *CYP3A4*1G* GA HepG2 cells was lower than those in *CYP3A4*1G* GG ($P < 0.01$) and AA HepG2 cells ($P < 0.05$), while there was no significant difference between *CYP3A4*1G* AA and GG HepG2 cells (Fig. 6B).

Discussion

CYP3A plays a critical role in the metabolism of drugs and other exogenous and endogenous substances, and its function is modified by genetic factors (Zhai et al., 2022). *CYP3A4*1G* affects drug metabolisms by altering *CYP3A4* expression and enzyme activity in vivo and in human liver tissues (Miura et al., 2011; He et al., 2014; Yuan et al., 2015). Our previous study showed *CYP3A4*1G* as an enhancer, regulating *CYP3A4* expression indirectly in an allele-dependent manner (Yang et al., 2015). Until now, due mainly to the lack of validated *CYP3A4*1G* cell models, it was not clear whether the *CYP3A4*1G* variant could regulate *CYP3A4* expression and metabolism in gene-edited cells. Therefore, in this study, we constructed the homozygous point mutations *CYP3A4*1G* GG and AA in HepG2 cells using CRISPR/Cas9. These *CYP3A4*1G* HepG2 cells may provide cell models for studying the molecular mechanism by which *CYP3A4*1G* regulates *CYP3A4* and *CYP3A5* expression, and through further CRISPR/Cas9-induced SNPs, provide a means to research the mechanisms of *CYP3A5*3*, or its linkage with *CYP3A4*1G*, in regulating *CYP3A5*.

Our results showed that *CYP3A4*1G* regulates basal expression of *CYP3A4* mRNA and protein, in an allele-dependent manner (Fig. 4, A and B), and that *CYP3A4* expression in *CYP3A4*1G* AA HepG2 cells is lower than that in *CYP3A4*1G* GG HepG2 cells. These findings further support our previous in vitro luciferase enhancer reporter assays, which showed the *CYP3A4*1G* A allele has a lower enhancer activity than *CYP3A4*1G* G allele in a reverse orientation (Yang et al., 2015). Moreover, the results are consistent with studies in liver microsomes (Yuan et al., 2015) and pharmacokinetic studies among *CYP3A5* expressers (Miura et al., 2011; Liu et al., 2017). For example, Miura et al. suggested that *CYP3A4*1G* A allele carriers are related to the lower dose-adjusted area under the concentration-time curve (0–12) of tacrolimus than those with the *CYP3A4*1G* GG genotype among *CYP3A5*

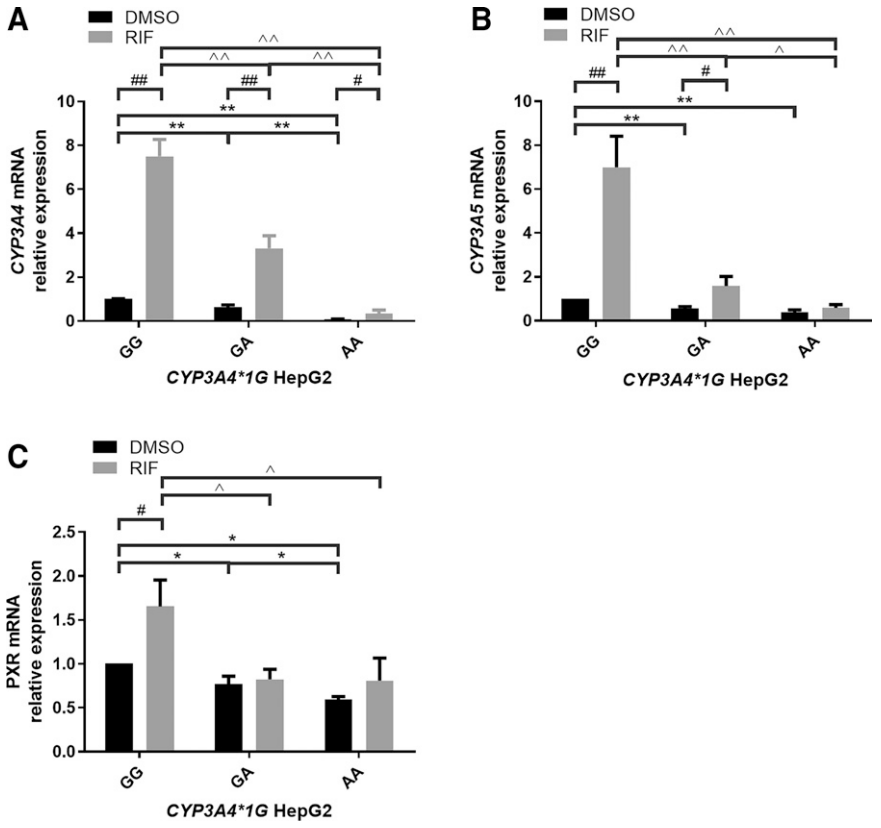

Fig. 5. *CYP3A* induction expression by RIF in *CYP3A4*1G* GG, GA, and AA HepG2 cells. *CYP3A* (A, B) and *PXR* (C) mRNA expression in *CYP3A4*1G* GG, GA, and AA HepG2 cells after 48 h induced by rifampicin (RIF). DMSO group for control. The error bars represent S.D. (n = 3 per group for mRNA). (*$P < 0.05$, **$P < 0.01$ versus GG or GA control group; $^{\#}P < 0.05$, $^{\#\#}P < 0.01$ versus the same genotype control group; ^$P < 0.05$, ^^$P < 0.01$ versus GG or GA RIF group).

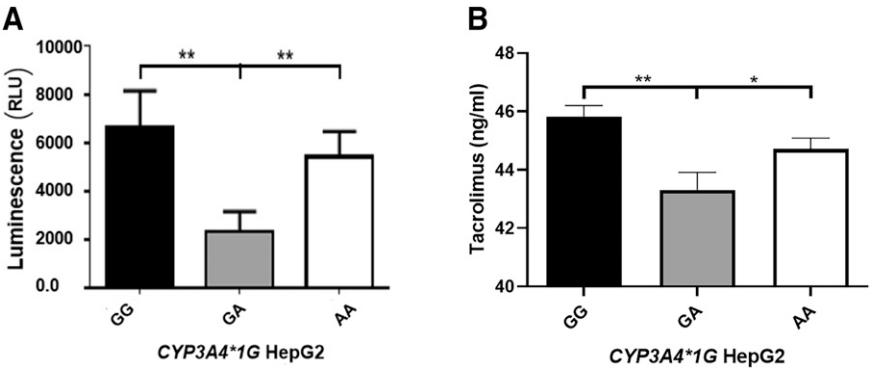

Fig. 6. CYP3A4 enzyme activity and tacrolimus metabolism study in *CYP3A4*1G* GG, GA, and AA HepG2 cells. CYP3A4 enzyme activity levels (A) and tacrolimus metabolism study (B) in *CYP3A4*1G* GG, GA, and AA HepG2 cells. The amount of tacrolimus metabolized in *CYP3A4*1G* GG, GA, and AA HepG2 cells is shown. (n = 3 per group for CYP3A4 enzyme activity and tacrolimus metabolism). The error bars represent S.D. (*$P < 0.05$, **$P < 0.01$).

expressers, but not *CYP3A5* non-expressers (Miura et al., 2011). Moreover, among *CYP3A5* non-expressers, He et al. also showed *CYP3A4*1G* AA and GA groups have lower area under the concentration-time curve (0–∞) versus the *CYP3A4*1G GG* group (He et al., 2014). Importantly, to better understand the molecular mechanism of the *CYP3A4*1G* enhancer's regulation of *CYP3A4* through transcription factor binding, studies using these *CYP3A4*1G* HepG2 cell models should be conducted in the future.

Similar to *CYP3A4*, *CYP3A4*1G* also regulates basal expression of *CYP3A5* indifferent *CYP3A4*1G* genotype HepG2 cells (Fig. 4, C and D). It may be because of the strong linkage relation between the *CYP3A5*3* G variant allele and *CYP3A4*1G* G wildtype allele as well as *CYP3A5*3* A wildtype allele and *CYP3A4*1G* A variant allele (Uesugi et al., 2013; Qi et al., 2022). We believe the lower *CYP3A5* expression shown by *CYP3A4*1G* AA HepG2 cells, compared with the *CYP3A4*1G* GG and GA HepG2 cells, is a result of the *CYP3A5*3* G allele forming a new linkage with the *CYP3A4*1G* A allele, which replaces the primary G wild-type allele and *CYP3A4*1G* A allele, having lower enhancer activity than the *CYP3A4*1G* G allele. Conversely, in *CYP3A4*1G* GG HepG2 cells, as the *CYP3A5*3* A wild-type allele forms a new linkage with the *CYP3A4*1G* G wild-type allele (which replaces the primary A variant allele), and *CYP3A4*1G* G allele has a higher enhancer activity than *CYP3A4*1G* A allele, this results in *CYP3A4*1G* GG HepG2 cells having higher *CYP3A5* expression than the other *CYP3A4*1G* genotype HepG2 cells. Similar to our study, Dorr et al., used CRISPR/Cas9 to confirm the *CYP3A5*3* A allele increased *CYP3A5* expression, furthering the metabolism of midazolam and tacrolimus by editing *CYP3A5*3 GG* into AA and AG genotype in Huh7 cells carrying *CYP3A4*1G* GA and *CYP3A4*22* CC genotypes (Dorr et al., 2017). Another study revealed that *CYP3A4*1G* A allele acts as a marker for the *CYP3A5*3* A allele, which increases tacrolimus clearance in Japanese liver transplant patients (Uesugi et al., 2013), also supporting the regulatory relationship of *CYP3A4*1G* and *CYP3A5*3* in our present study.

Accordingly, through CYP3A4 and CYP3A5 metabolic functional studies, we also found that *CYP3A4*1G* decreases CYP3A4 enzyme activity and tacrolimus metabolism in *CYP3A4*1G* GA HepG2 cells. This finding is similar to previous results that dose-adjusted C_0 in *CYP3A4*1G* carriers is lower than *CYP3A4*1G* GG individuals in *CYP3A5* expressers (Miura et al., 2011). Enzyme activity may be affected by post-transcriptional regulation (protein expression) or post-translational modifications (phosphorylation, etc.). *CYP3A4*1G* affecting CYP3A4 enzyme is partly different from its role for *CYP3A4* expression; it is suspected that multisite phosphorylation of CYP3A4 is associated with enhancing its gp78- and CHIP-mediated ubiquitination (Wang et al., 2012; Kwon et al., 2019).

Taken together, our results show that *CYP3A4*1G* regulates basal expression and enzyme activity of *CYP3A4* and *CYP3A5* in different *CYP3A4*1G* genotype HepG2 cells with the *CYP3A5*3* AG genotype. Lin et al. found that, in people with the *CYP3A5*3* AG genotype, there is a certain correlation between *CYP3A4* and *CYP3A5* protein and mRNA, and speculated there may be conserved 5′-flanking region elements involved in constitutive expression of *CYP3A4* and *CYP3A5* through sharing a common regulatory pathway (Lin et al., 2002). In agreeance with this, in HepG2 cells with *CYP3A5*3* AG genotype, we found that *CYP3A4*1G*, as an enhancer, regulates expression of *CYP3A4* and *CYP3A5*. In addition, Collins and Wang proposed that *CYP3A4*1G* downregulates *CYP3A4* and *CYP3A5* expression through a lncRNA, AC069294.1 (Collins and Wang, 2022). Further validation will be done in these various *CYP3A4*1G* different HepG2 cells. *CYP3A4*1G* decreases CYP3A4 enzyme activity and tacrolimus metabolism in *CYP3A4*1G* GA HepG2 cells, revealing that individuals with *CYP3A5*3* AG and *CYP3A4*1G* GA genotype, requires a lower dose of tacrolimus than those with *CYP3A5*3* AG and *CYP3A4*1G* GG or AA genotype.

We also found that *CYP3A4*1G* regulates the RIF-induced expression of *CYP3A4* and *CYP3A5* in a *CYP3A4*1G* allele-dependent manner in HepG2 cells (Fig. 5, A and B). It is well known that RIF increases expression of *CYP3A4* by regulating the transcription factor PXR. Meanwhile, we found that *CYP3A4*1G* may also affect *PXR* expression. Therefore, we believe that *CYP3A4*1G* and RIF act together on PXR to regulate *CYP3A4* and *CYP3A5* expression. As to the relation of *CYP3A5* expression and RIF, our results are consistent with the Burk group's suggestion that in liver tissue, RIF-induced *CYP3A5* expression may phenocopy the effects of the *CYP3A5*3* A, a high expression allele (Burk et al., 2004). Barwick et al. and Burk et al. found that RIF inductions of *CYP3A4* and *CYP3A5* share a similar mechanism in which the induction is mediated by the proximal everted repeat sequence separated by 6 bp (ER6) binding site for PXR in the promoter of *CYP3A4* or *CYP3A5* (Barwick et al., 1996; Burk et al., 2004). This still leads to two speculations. In combination with RIF, *CYP3A4*1G* enhances expression of *CYP3A4* or *CYP3A5* by PXR and its ER6-regulatory element in the *CYP3A4* or *CYP3A5* proximal 5′promoter. Furthermore, *CYP3A4*1G* alone can also enhance expression of *CYP3A4* or *CYP3A5* through PXR and its ER6 regulatory element in *CYP3A4* or *CYP3A5* proximal 5′promoter. Thus, further studies using *CYP3A4*1G* HepG2 cells, with or without RIF, are required to elucidate the molecular mechanisms by which *CYP3A4*1G*, as an enhancer, regulates *CYP3A4* or *CYP3A5* expression through PXR binding the ER6 regulatory element in the *CYP3A4* or *CYP3A5* proximal 5′promoter.

There are some limitations in this study. There is no data showing how *CYP3A4*1G* GG, GA, and AA genotypes affect the actual drug metabolism of CYP3A4 substrates. Furthermore, similar to other CRISPR/Cas9 edited cells, in these point mutation *CYP3A4*1G* GG and AA HepG2 cells, there are also a few base deletions in *CYP3A4* intron 10 near *CYP3A4*1G* site. There are also a few base substitutions/insertions and deletions of 14 bases near the location of off-targets on

chr7 of *CYP3A7* gene far away from *CYP3A4*, although they have no obvious effects on the *CYP3A4*1G* regulated *CYP3A4* and *CYP3A5* expression, or combination with RIF treatment, in the present study.

In conclusion, we constructed *CYP3A4*1G* GG and AA point mutation HepG2 cell strains, and found *CYP3A4*1G* regulating both basal and RIF-induced expression and enzyme activity of *CYP3A4* and *CYP3A5*. These findings will provide a new theoretical basis for clinical precision therapy based on *CYP3A4*1G* as a biomarker. Considering the linkage relation of *CYP3A4*1G* and *CYP3A5*3*, and complex of CYP3A substrates, use of *CYP3A4*1G*, *CYP3A5*3,* and *CYP3A4*22* as biomarkers is recommended to guide CYP3A precision therapy.

Authorship Contributions

Participated in research design: Yang, Zhao, Z. Zhang, L.R. Zhang.

Conducted experiments: Yang, Zhao, Dou, Chang, Xu.

Performed data analysis: Yang, Zhao, Dou, Xu.

Wrote or contributed to the writing of the manuscript: Yang, Zhao, P. Wang, Chang, Qiao, X. Wang, L.R. Zhang.

References

Barwick JL, Quattrochi LC, Mills AS, Potenza C, Tukey RH, and Guzelian PS (1996) Trans-species gene transfer for analysis of glucocorticoid-inducible transcriptional activation of transiently expressed human CYP3A4 and rabbit CYP3A6 in primary cultures of adult rat and rabbit hepatocytes. *Mol Pharmacol* **50**:10–16.

Bu Y and Gelman IH (2007) v-Src-mediated down-regulation of SSeCKS metastasis suppressor gene promoter by the recruitment of HDAC1 into a USF1-Sp1-Sp3 complex. *J Biol Chem* **282**:26725–26739.

Burk O, Koch I, Raucy J, Hustert E, Eichelbaum M, Brockmöller J, Zanger UM, and Wojnowski L (2004) The induction of cytochrome P450 3A5 (CYP3A5) in the human liver and intestine is mediated by the xenobiotic sensors pregnane X receptor (PXR) and constitutively activated receptor (CAR). *J Biol Chem* **279**:38379–38385.

Collins JM and Wang D (2022) Regulation of CYP3A4 and CYP3A5 by a lncRNA: a potential underlying mechanism explaining the association between CYP3A4*1G and CYP3A metabolism. *Pharmacogenet Genomics* **32**:16–23.

Dong ZL, Li H, Chen QX, Hu Y, Wu SJ, Tang LY, Gong WY, Xie GH, and Fang XM (2012) Effect of CYP3A4*1G on the fentanyl consumption for intravenous patient-controlled analgesia after total abdominal hysterectomy in Chinese Han population. *J Clin Pharm Ther* **37**:153–156.

Dorr CR, Remmel RP, Muthusamy A, Fisher J, Moriarity BS, Yasuda K, Wu B, Guan W, Schuetz EG, Oetting WS et al. (2017) CRISPR/Cas9 Genetic Modification of *CYP3A5 *3* in HuH-7 Human Hepatocyte Cell Line Leads to Cell Lines with Increased Midazolam and Tacrolimus Metabolism. *Drug Metab Dispos* **45**:957–965.

Gao Y, Zhang LR, and Fu Q (2008) CYP3A4*1G polymorphism is associated with lipid-lowering efficacy of atorvastatin but not of simvastatin. *Eur J Clin Pharmacol* **64**:877–882.

He BX, Shi L, Qiu J, Tao L, Li R, Yang L, and Zhao SJ (2011) A functional polymorphism in the CYP3A4 gene is associated with increased risk of coronary heart disease in the Chinese Han population. *Basic Clin Pharmacol Toxicol* **108**:208–213.

He BX, Shi L, Qiu J, Zeng XH, and Zhao SJ (2014) The effect of CYP3A4*1G allele on the pharmacokinetics of atorvastatin in Chinese Han patients with coronary heart disease. *J Clin Pharmacol* **54**:462–467.

Hegde N, Joshi S, Soni N, and Kushalappa AC (2021) The caffeoyl-CoA O-methyltransferase gene SNP replacement in Russet Burbank potato variety enhances late blight resistance through cell wall reinforcement. *Plant Cell Rep* **40**:237–254.

Kato M, Zhang J, Wang M, Lanting L, Yuan H, Rossi JJ, and Natarajan R (2007) MicroRNA-192 in diabetic kidney glomeruli and its function in TGF-beta-induced collagen expression via inhibition of E-box repressors. *Proc Natl Acad Sci USA* **104**:3432–3437.

Kuehl P, Zhang J, Lin Y, Lamba J, Assem M, Schuetz J, Watkins PB, Daly A, Wrighton SA, Hall SD et al. (2001) Sequence diversity in CYP3A promoters and characterization of the genetic basis of polymorphic CYP3A5 expression. *Nat Genet* **27**:383–391.

Kwon D, Kim SM, Jacob P, Liu 3rd Y, and Correia MA (2019) Induction via Functional Protein Stabilization of Hepatic Cytochromes P450 upon gp78/Autocrine Motility Factor Receptor (AMFR) Ubiquitin E3-Ligase Genetic Ablation in Mice: Therapeutic and Toxicological Relevance. *Mol Pharmacol* **96**:641–654.

Lin YS, Dowling AL, Quigley SD, Farin FM, Zhang J, Lamba J, Schuetz EG, and Thummel KE (2002) Co-regulation of CYP3A4 and CYP3A5 and contribution to hepatic and intestinal midazolam metabolism. *Mol Pharmacol* **62**:162–172.

Liu MZ, He HY, Zhang YL, Hu YF, He FZ, Luo JQ, Luo ZY, Chen XP, Liu ZQ, Zhou HH et al. (2017) IL-3 and CTLA4 gene polymorphisms may influence the tacrolimus dose requirement in Chinese kidney transplant recipients. *Acta Pharmacol Sin* **38**:415–423.

Liu H, Jing Y, Zou D, Hou X, Peng H, Zhou J, Li Y, Xiong D, Wen J, and Wei X (2020) Regulation of indirubin derivative PHII-7 on tacrolimus transport and metabolism via PXR-CYP3 A5/ABCB1 signaling pathway and its mechanism. *Zhongguo Yaolixue Tongbao* **36**:927–934.

López-Terrada D, Cheung SW, Finegold MJ, and Knowles BB (2009) Hep G2 is a hepatoblastoma-derived cell line. *Hum Pathol* **40**:1512–1515.

Lv J, Liu F, Feng N, Sun X, Tang J, Xie L, and Wang Y (2018) CYP3A4 gene polymorphism is correlated with individual consumption of sufentanil. *Acta Anaesthesiol Scand* **62**:1367–1373.

Miura M, Satoh S, Kagaya H, Saito M, Numakura K, Tsuchiya N, and Habuchi T (2011) Impact of the CYP3A4*1G polymorphism and its combination with CYP3A5 genotypes on tacrolimus pharmacokinetics in renal transplant patients. *Pharmacogenomics* **12**:977–984.

Mulder TAM, van Eerden RAG, de With M, Elens L, Hesselink DA, Matic M, Bins S, Mathijssen RHJ, and van Schaik RHN (2021) *CYP3A4*22* Genotyping in Clinical Practice: Ready for Implementation? *Front Genet* **12**:711943.

Pande P, Zhong XB, and Ku WW (2020) Histone Methyltransferase G9a Regulates Expression of Nuclear Receptors and Cytochrome P450 Enzymes in HepaRG Cells at Basal Level and in Fatty Acid Induced Steatosis. *Drug Metab Dispos* **48**:1321–1329.

Qi G, Han C, Zhou Y, and Wang X (2022) Allele and genotype frequencies of CYP3A4, CYP3A5, CYP3A7, and GSTP1 gene polymorphisms among mainland Tibetan, Mongolian, Uyghur, and Han Chinese populations. *Clin Exp Pharmacol Physiol* **49**:219–227.

Ren ZY, Xu XQ, Bao YP, He J, Shi L, Deng JH, Gao XJ, Tang HL, Wang YM, and Lu L (2015) The impact of genetic variation on sensitivity to opioid analgesics in patients with postoperative pain: a systematic review and meta-analysis. *Pain Physician* **18**:131–152.

Shi C, Yan L, Gao J, Chen S, and Zhang L (2022) Effects of ABCB1 DNA methylation in donors on tacrolimus blood concentrations in recipients following liver transplantation. *Br J Clin Pharmacol* **88**:4505–4514.

Tang J, Xu J, Zhang YL, Liu R, Liu MZ, Hu YF, Shao MJ, Zhu LJ, Cao S, Xin HW et al. (2019) Incorporation of Gene-Environment Interaction Terms Improved the Predictive Accuracy of Tacrolimus Stable Dose Algorithms in Chinese Adult Renal Transplant Recipients. *J Clin Pharmacol* **59**:890–899.

Uesugi M, Hosokawa M, Shinke H, Hashimoto E, Takahashi T, Kawai T, Matsubara K, Ogawa K, Fujimoto Y, Okamoto S et al. (2013) Influence of cytochrome P450 (CYP) 3A4*1G polymorphism on the pharmacokinetics of tacrolimus, probability of acute cellular rejection, and mRNA expression level of CYP3A5 rather than CYP3A4 in living-donor liver transplant patients. *Biol Pharm Bull* **36**:1814–1821.

Wang D, Chen H, Momary KM, Cavallari LH, Johnson JA, and Sadée W (2008) Regulatory polymorphism in vitamin K epoxide reductase complex subunit 1 (VKORC1) affects gene expression and warfarin dose requirement. *Blood* **112**:1013–1021.

Wang D, Guo Y, Wrighton SA, Cooke GE, and Sadee W (2011) Intronic polymorphism in CYP3A4 affects hepatic expression and response to statin drugs. *Pharmacogenomics J* **11**:274–286.

Wang D and Sadee W (2016) CYP3A4 intronic SNP rs35599367 (CYP3A4*22) alters RNA splicing. *Pharmacogenet Genomics* **26**:40–43.

Wang Y, Guan S, Acharya P, Liu Y, Thirumaran RK, Brandman R, Schuetz EG, Burlingame AL, and Correia MA (2012) Multisite phosphorylation of human liver cytochrome P450 3A4 enhances Its gp78- and CHIP-mediated ubiquitination: a pivotal role of its Ser-478 residue in the gp78-catalyzed reaction. *Mol Cell Proteomics* **11**:M111.010132.

Yang W, Zhao D, Han S, Tian Z, Yan L, Zhao G, Kan Q, Zhang W, and Zhang L (2015) CYP3A4*1G regulates CYP3A4 intron 10 enhancer and promoter activity in an allelic-dependent manner. *Int J Clin Pharmacol Ther* **53**:647–657.

Yuan JJ, Hou JK, Zhang W, Chang YZ, Li ZS, Wang ZY, Du YY, Ma XJ, Zhang LR, Kan QC et al. (2015) CYP3A4 * 1G Genetic Polymorphism Influences Metabolism of Fentanyl in Human Liver Microsomes in Chinese Patients. *Pharmacology* **96**:55–60.

Yuan R, Zhang X, Deng Q, Wu Y, and Xiang G (2011) Impact of CYP3A4*1G polymorphism on metabolism of fentanyl in Chinese patients undergoing lower abdominal surgery. *Clin Chim Acta* **412**:755–760.

Zhai Q, van der Lee M, van Gelder T, and Swen JJ (2022) Why We Need to Take a Closer Look at Genetic Contributions to CYP3A Activity. *Front Pharmacol* **13**:912618.

Zhang H, Chen M, Wang X, and Yu S (2017) Patients with CYP3A4*1G genetic polymorphism consumed significantly lower amount of sufentanil in general anesthesia during lung resection. *Medicine (Baltimore)* **96**:e6013.

Zhang J, Zhang L, Zhao X, Shen S, Luo X, and Zhang Y (2018) Association between MDR_1 /CYP3A4/$OPRM_1$ gene polymorphisms and the post-caesarean fentanyl analgesic effect on Chinese women. *Gene* **661**:78–84.

Zhang W, Chang YZ, Kan QC, Zhang LR, Li ZS, Lu H, Wang ZY, Chu QJ, and Zhang J (2010) CYP3A4*1G genetic polymorphism influences CYP3A activity and response to fentanyl in Chinese gynecologic patients. *Eur J Clin Pharmacol* **66**:61–66.

Zhao YLYW and Zhang LR (2016) Genotype analysis of CYP3A, SLCO1B1 and POR in HepG2 cells. *Journal of Zhengzhou University* **51**:583–587 Medical Sciences.

Address correspondence to: Dr. Lirong Zhang, Department of Pharmacology, School of Basic Medical Sciences, Zhengzhou University, Zhengzhou, Henan, China. E-mail: zhanglirongzzu@126.com

Supplemental Figure 1

A

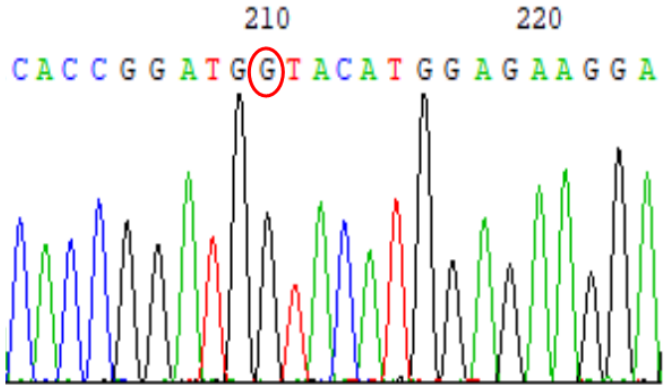

px330-2W

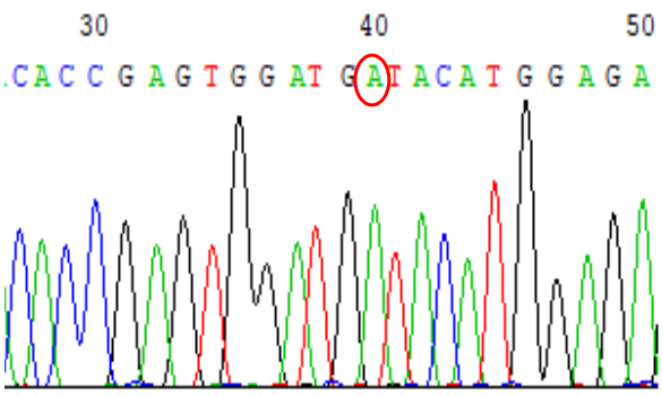

px330-3M

B

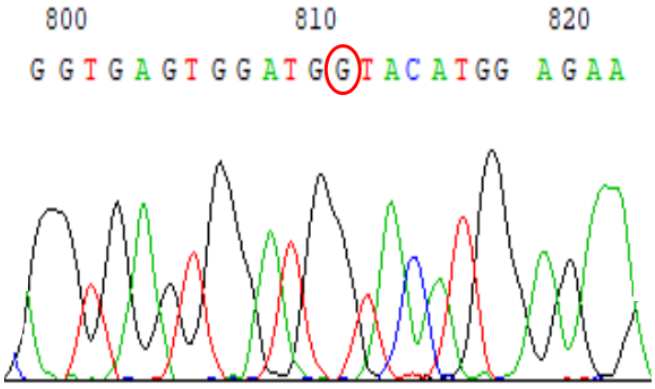

reporter-W

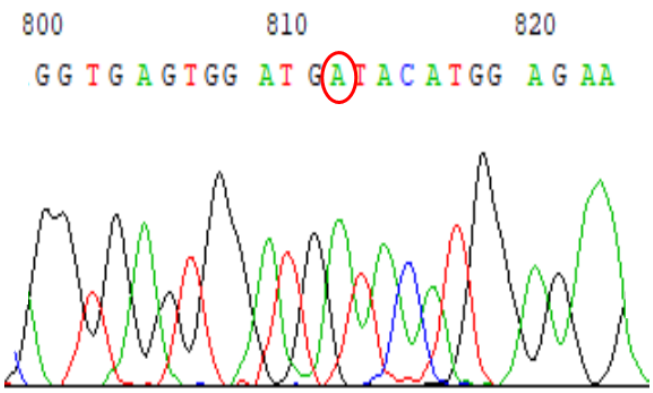

reporter-M

C

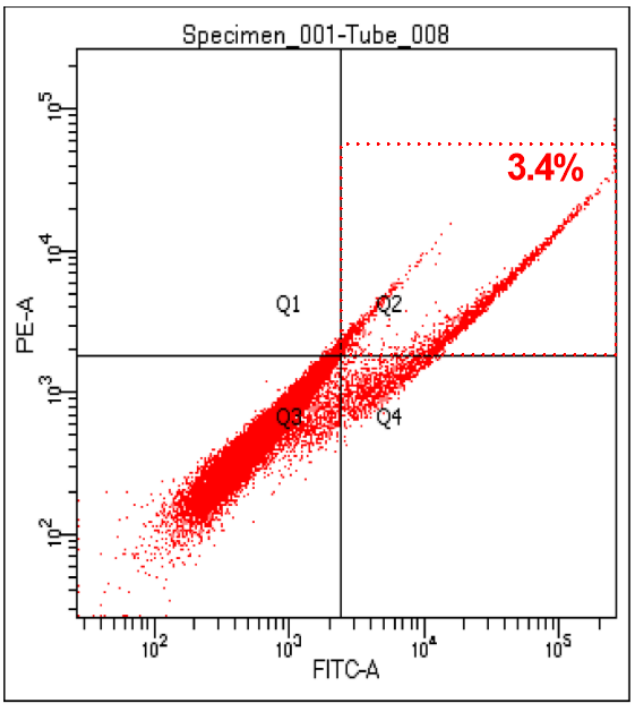

px330-2W

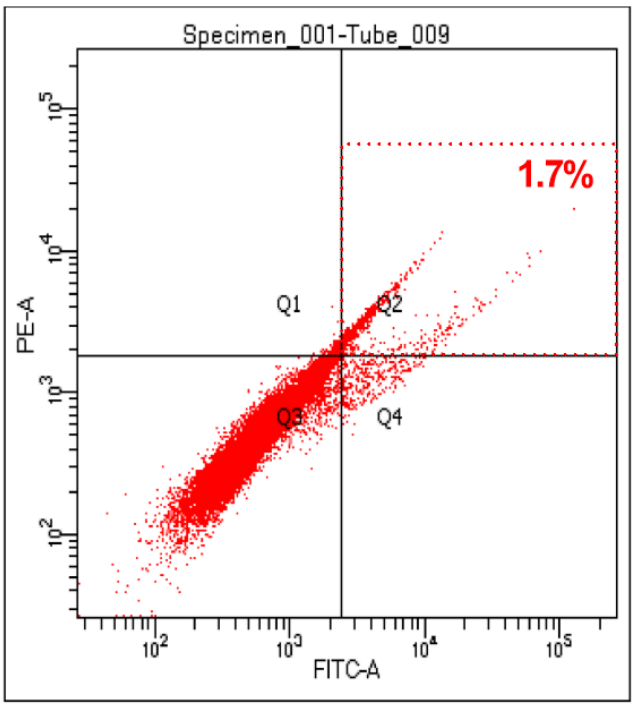

px330-3M

Supplemental Figure 2

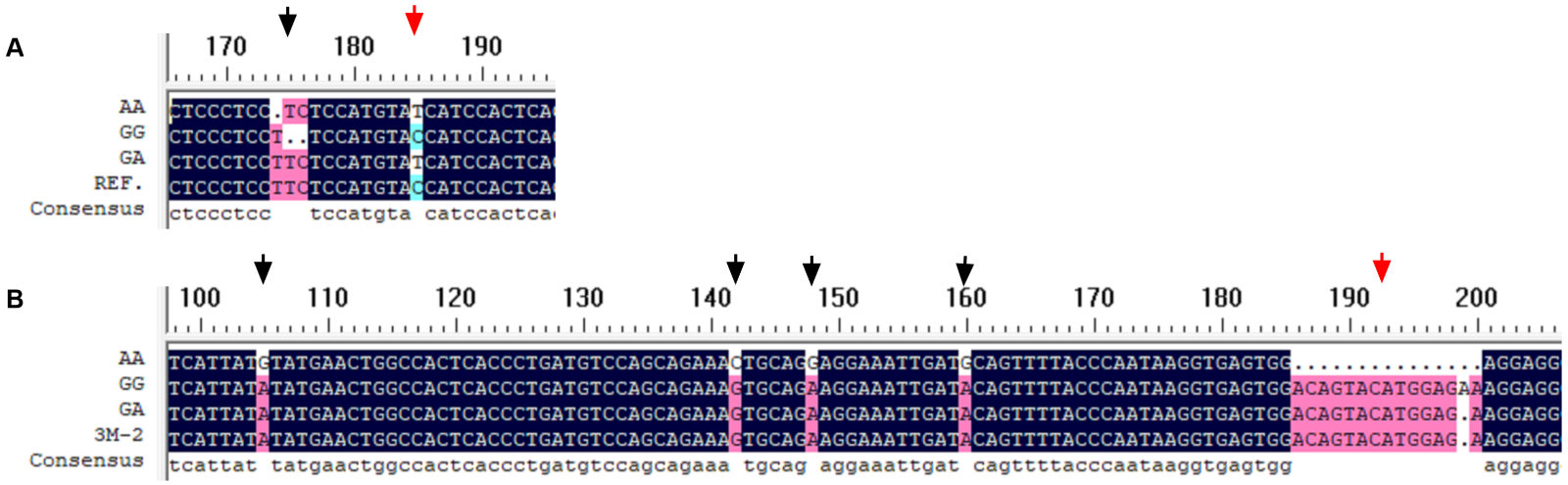

Supplemental Figure 3

A

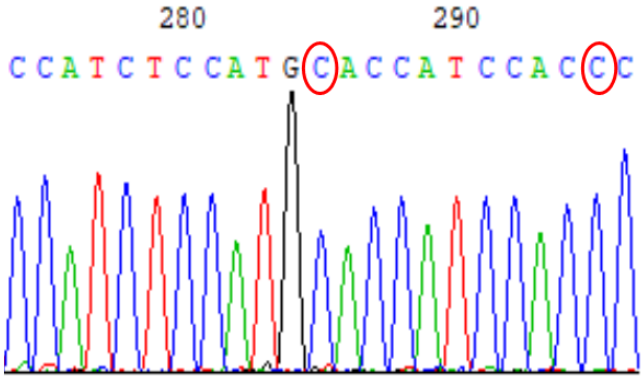

chr7:+36250405

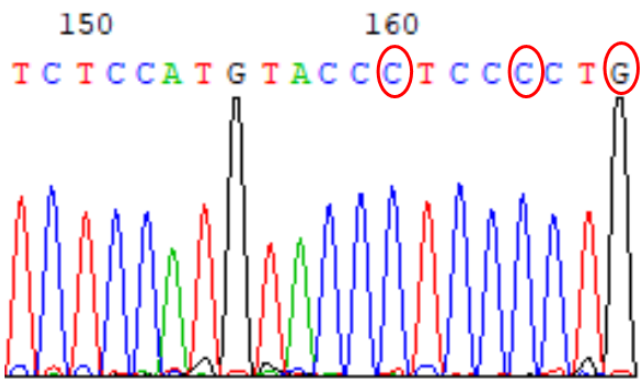

chr2: +104879416

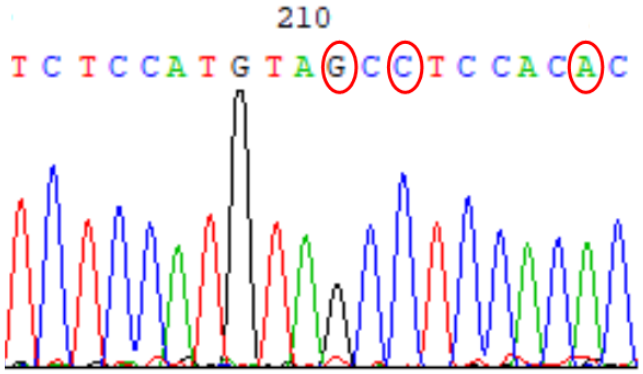

chr8: -64260441

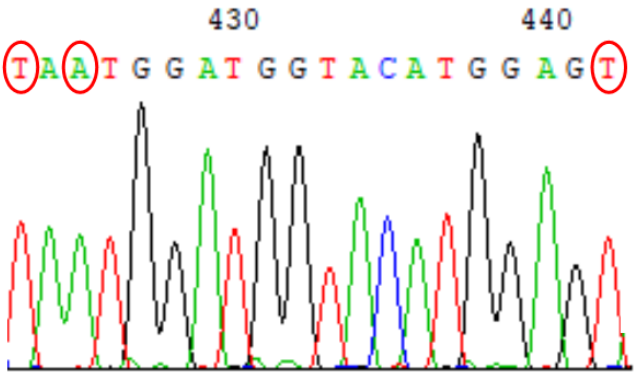

chr6: +24425984

B

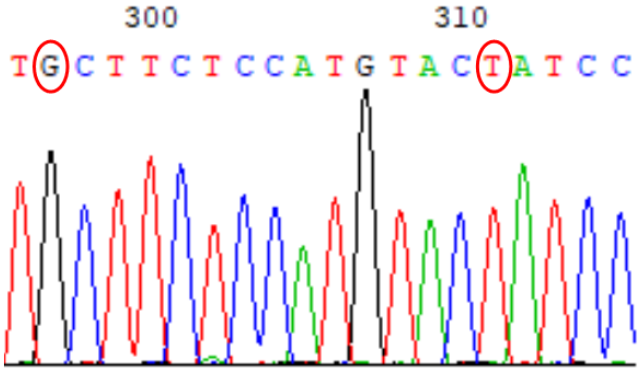

chr17: +42725810

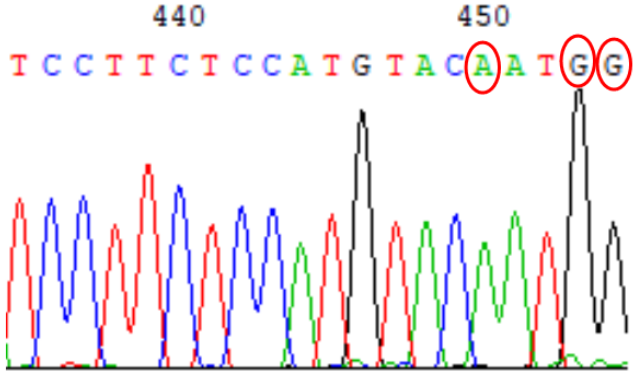

chr10: -23770060

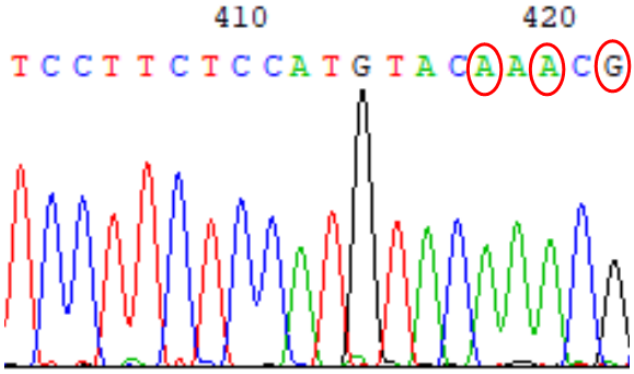

chr4: +187178998

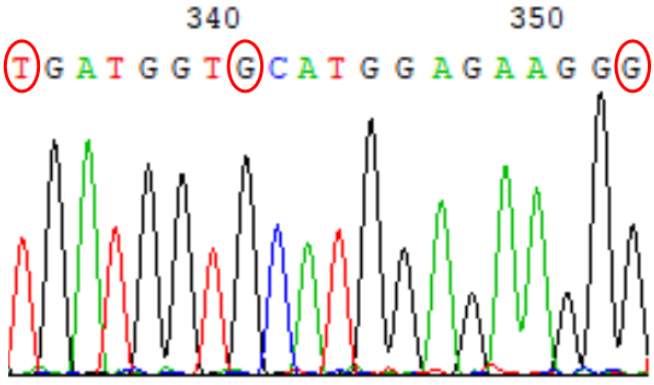

chr11: -132777040

SUPPLEMENTARY MATERIALS

CYP3A4 and *CYP3A5* expression is regulated by C*YP3A4*1G* in CRISPR/Cas9 edited HepG2 cells

Weihong Yang, Huan Zhao, Yaojie Dou, Pei Wang, Qi Chang, Xiaomeng Qiao, Xiaofei Wang, Chen Xu, Zhe Zhang, Lirong Zhang

DMD-AR-2022-001111

Supplemental Table 1: sgRNA, pmCherry EGFP reporter and template sequence

Primers	Sequence (5'- 3')
*CYP3A4*1G* sg-2W F	CACCggatggtacatggagaagga
*CYP3A4*1G* sg-2W R	AAACtccttctccatgtaccatcc
*CYP3A4*1G* sg-3M F	CACCgagtggatgatacatggaga
*CYP3A4*1G* sg-3M R	AAACtctccatgtatcatccactc
reporter-*1G W F	TCGACaggtgagtggatggtacatggagaaggagggaggaTAAC
reporter-*1G W R	AATTGTTAtcctccctccttctccatgtaccatccactcacctG
reporter-*1G M F	TCGACaggtgagtggatgatacatggagaaggagggaggaTAAC
reporter-*1G M R	AATTGTTAtcctccctccttctccatgtatcatccactcacctG
*1G ssODN1 (G>A) template	tgtccagcagaaactgcaggaggaaattgatgcagttttacccaataaggtgagt ggatgatacatggagaaggagggaggaggtgaaaccttagcaaaaatgcctcct caccacttccca
*1G ssODN2 (A>G) template	tgtccagcagaaactgcaggaggaaattgatgcagttttacccaataaggtgagt ggatggtacatggagaaggagggaggaggtgaaaccttagcaaaaatgcctcc tcaccacttccca

Notes: sg-2W and sg-3M indicate sgRNA of wild allele and mutation allele, respectively. Red lowercase letter in the table S1 indicates *CYP3A4*1G* site. Reporter-*1G W/M indicate pmCherry EGFP reporter of *CYP3A4*1G* wild allele/mutation allele. F/R indicates forward/reverse primer. 'CACC' and 'AAAC' are sticky ends of cleavage site for the restriction endonuclease BbsI. 'TCGAC', 'AATTG', 'G', 'C', 'TAA' and red bases are sticky ends of EcoRI or XhoI, terminator codon sequence, modified bases

in the terminal ends of these enzymes' sticky ends.

Supplemental Table 2: PCR primer sequence for identifying monoclonal HepG2 cell strains and primers for qRT-PCR

Primers	Sequence (5'- 3')
*CYP3A4*1G* F	CACCCTGATGTCCAGCAGAAACT
*CYP3A4*1G* R	AATAGAAAGCAGATGAACCAGAGCC
GAPDH mRNA F	GTCAGTGGTGGACCTGACCT
GAPDH mRNA R	TGAGCTTGACAAAGTGGTCG
CYP3A4 mRNA F	CACAGATCCCCCTGAAATTAAGCTTA
CYP3A4 mRNA R	AAAATTCAGGCTCCACTTACGGTG
CYP3A5 mRNA F	TGTTATTCTGTCTTCACAAATCGAA
CYP3A5 mRNA R	CCTCAAGTTTCTCACCAATACATCT
PXR mRNA F	CAACCTACATGTTCAAAGGCATC
PXR mRNA R	ACACTCCCAGGTTCCAGTCTC

Notes: F and R represent forward and reverse primer, respectively.

Supplemental Table 3: Off-target gene sequence, location on chromosome and primers of off-target location for *CYP3A4*1G* sgRNA-2W, sgRNA-3M

Gene sequence	location on chromosome	Primers	Sequence (5'- 3')
GGACAGTACATGGAGAAGGA*	chr7: -99710709	2W-1 F	CTGGGAAGTGGTGAGGAA
		2W-1 R	TGTGAAGGTGGCAGGGAT
GGATAGTACATGGAGAAGCA*	chr17: +42725810	2W-2 F	GGGACTCTTATTCACCTTTG
		2W-2 R	GGCTGTGACAGGTGGATC
CCATTGTACATGGAGAAGGA*	chr10: -23770060	2W-3 F	AGTTCAGCCGATGTCCAG
		2W-3 R	ATGGTAACCACCAAGTAGGG
CGTTTGTACATGGAGAAGGA*	chr4: +187178998	2W-4 F	GCATCATTCCTGCTGGTCAT
		2W-4 R	CTCAGCAACAATTTCCACCA
TGATGGTGCATGGAGAAGGG*	chr11: -132777040	2W-5 F	TATCCAGCATCACATATTCCT
		2W-5 R	CTTTATTTCACCCTCCTTACA

GGGTGGATGGTGCATGGAGA#	chr7: +36250405	3M-1 F	CTGGGCAACATAGTGAAACC
		3M-1 R	CAGACAATAAGTTGAATGGGTA
GAGTGGACAGTACATGGAGA#	chr7: -99710713	3M-2 F	CTGGGAAGTGGTGAGGAA
		3M-2 R	TGTGAAGGTGGCAGGGAT
CAGGGGAGGGTACATGGAGA#	chr2: +104879416	3M-3 F	ACCACACACATACAGATGGAGAG
		3M-3 R	TGAAGAGATGCTGCAGGAA
GTGTGGAGGCTACATGGAGA#	chr8: -64260441	3M-4 F	TAGACCTGCCCATCATCAAC
		3M-4 R	CGGGTAGTATTGGCGGAG
TAATGGATGGTACATGGAGT#	chr6: +24425984	3M-5 F	GTGATTGCAGGATGCTTCTTA
		3M-5 R	AGACCTTACCTTGTAGGGTTG